A novel endocytic pathway induced by clustering endothelial ICAM-1 or PECAM-1

Silvia Muro[2,4], Rainer Wiewrodt[3], Anu Thomas[2,4], Lauren Koniaris[3,4], Steven M. Albelda[3], Vladimir R. Muzykantov[2,4,*] and Michael Koval[1,4,*]

[1]Departments of Physiology, [2]Pharmacology and Medicine, Pulmonary and [3]Critical Care Division and [4]Institute for Environmental Medicine, University of Pennsylvania School of Medicine, B-400 Richards/6085, 3700 Hamilton Walk, Philadelphia, PA 19104, USA

*Authors for correspondence (e-mail: mkoval@mail.med.upenn.edu, muzykant@mail.med.upenn.edu)

Accepted 14 February 2003
Journal of Cell Science 116, 1599-1609 © 2003 The Company of Biologists Ltd
doi:10.1242/jcs.00367

Summary

Antibody conjugates directed against intercellular adhesion molecule (ICAM-1) or platelet-endothelial cell adhesion molecule (PECAM-1) have formed the basis for drug delivery vehicles that are specifically recognized and internalized by endothelial cells. There is increasing evidence that ICAM-1 and PECAM-1 may also play a role in cell scavenger functions and pathogen entry. To define the mechanisms that regulate ICAM-1 and PECAM-1 internalization, we examined the uptake of anti-PECAM-1 and anti-ICAM-1 conjugates by endothelial cells. We found that the conjugates must be multimeric, because monomeric anti-ICAM-1 and anti-PECAM-1 are not internalized. Newly internalized anti-ICAM-1 and anti-PECAM-1 conjugates did not colocalize with either clathrin or caveolin, and immunoconjugate internalization was not reduced by inhibitors of clathrin-mediated or caveolar endocytosis, suggesting that this is a novel endocytic pathway. Amiloride and protein kinase C (PKC) inhibitors, agents known to inhibit macropinocytosis, reduced the internalization of clustered ICAM-1 and PECAM-1. However, expression of dominant-negative dynamin-2 constructs inhibited uptake of clustered ICAM-1. Binding of anti-ICAM-1 conjugates stimulated the formation of actin stress fibers by human umbilical vein endothelial cells (HUVEC). Latrunculin, radicicol and Y27632 also inhibited internalization of clustered ICAM-1, suggesting that actin rearrangements requiring Src kinase and Rho kinase (ROCK) were required for internalization. Interestingly, these kinases are part of the signal transduction pathways that are activated when circulating leukocytes engage endothelial cell adhesion molecules, suggesting the possibility that CAM-mediated endocytosis is regulated using comparable signaling pathways.

Key words: HUVEC, Vascular endothelium, Cell adhesion, Macropinocytosis, Endocytosis

Introduction

Endothelial cells internalize natural ligands and artificial macromolecular ligands, that have been designed as carriers for specific drug and gene delivery (Danilov et al., 2001; Jacobson et al., 1996; McIntosh et al., 2002; Muzykantov et al., 1996; Spragg et al., 1997). We have previously shown that platelet-endothelial cell adhesion molecule (PECAM-1), an immunoglobulin superfamily cell adhesion molecule, can serve as a receptor for delivery of active enzymes and genetic materials to endothelial cells (Muzykantov et al., 1999; Scherpereel et al., 2001; Wiewrodt et al., 2002). Importantly, monomeric anti-PECAM-1 immunoglobulin G (IgG) and multivalent conjugates larger than 500 nm are not efficiently internalized; multivalent anti-PECAM-1 conjugates 100-300 nm in diameter are readily internalized, although molecular mechanisms that regulate the internalization of anti-PECAM-1 are not well understood (Wiewrodt et al., 2002).

It is becoming apparent that both PECAM-1 and ICAM-1 may serve as plasma membrane receptors to mediate internalization of natural ligands by different types of cells. For instance, coxsackieviruses and rhinoviruses bind ICAM-1 and are internalized (Shafren et al., 1997a), although other coreceptors may be involved in this process (Shafren et al., 1997b). HIV is internalized into brain endothelial cells by a pathway that is analogous to macropinocytosis into endocytic vesicles that also contain ICAM-1 (Liu et al., 2002). A pathway related to macropinocytosis has also been implicated in the clearance of apoptotic cell fragments by epithelial cells (Fiorentini et al., 2001). The notion that endothelial cells might help scavenge apoptotic cells is underscored by the observation that PECAM-1 is required for the binding of malaria-infected red blood cells to human umbilical vein endothelial cells (HUVEC) in culture (Treutiger et al., 1997), although these particles were too large to be endocytosed. In a recent study, PECAM-1 expressed by macrophages was found to play an important role in cellular recognition and uptake: apoptotic cells binding to macrophage PECAM-1 were efficiently phagocytosed, whereas live cells activated a signaling cascade through macrophage PECAM-1 to weaken their engagement to macrophages and enable their release (Brown et al., 2002). Cells, apoptotic fragments and viruses binding to ICAM-1 and PECAM-1 are multivalent, complex and, in the case of live cells, active partipicants in cell–cell interactions, making it difficult to discern roles for specific plasma membrane proteins as potential receptors. By contrast, anti-ICAM-1 and anti-PECAM-1 conjugates, although multivalent, will primarily engage only the cell adhesion molecule of interest, which makes them useful probes for

examining specific internalization pathways mediated by ICAM-1 or PECAM-1.

There are multiple pathways for ligand internalization involving vesicles 100-300 nm in diameter, including clathrin-mediated endocytosis and the clathrin-independent caveolae-mediated pathway (Mukherjee et al., 1997; Nichols and Lippincott-Schwartz, 2001). Each of these endocytic mechanisms differs in sensitivity to pharmacological agents, which enables the mechanism of ligand internalization to be determined. Caveolae-mediated endocytosis is a particularly important pathway in endothelial cells, where ligands such as albumin (Minshall et al., 2000) and orosomucoid (Predescu et al., 1998) are internalized via receptors clustered into caveolae and subsequently transcytosed across the endothelial barrier (McIntosh et al., 2002). There are also clathrin-independent pathways distinct from caveolar endocytosis, which mediate uptake of glycosylphosphatidylinositol (GPI)-anchored proteins, such as the folate receptor (Mayor et al., 1998) and diptheria toxin receptor (Skretting et al., 1999).

The regulation of ICAM-1 and PECAM-1 internalization by endothelial cells is not well understood at present. In particular, whether ICAM-1 and PECAM-1 are internalized by similar pathways is not known. In this study, we defined some key elements regulating the internalization of anti-ICAM-1 or anti-PECAM-1 conjugates by endothelial cells. In each case, clustering of the CAM was required for efficient internalization. Given that anti-ICAM-1 and anti-PECAM-1 conjugates did not colocalize with known endocytic coat proteins and from the analysis of the signaling pathways that regulate the uptake of anti-ICAM-1 and anti-PECAM-1 conjugates, our data suggests that that endothelial cells internalize clustered ICAM-1 and PECAM-1 using a novel endocytic pathway.

Materials and Methods

Reagents

Murine monoclonal antibodies to human ICAM-1 (R6.5) and PECAM-1 (mAb 62) were provided by Robert Rothlein (Boehringer-Ingelheim, Ridgefield, CN) and M. Nakada (Centocor, Malvern, PA), respectively. Control murine IgG was from Calbiochem (San Diego, CA). Anti-caveolin-1, anti-clathrin, anti-cholera toxin B and anti-transferrin were from Calbiochem (La Jolla, CA). Polyclonal rabbit anti-6-His-Tag was a gift from MBL (Nagoya, Japan). Secondary fluorescent antibodies were from Jackson ImmunoResearch (West Grove, PA) and Molecular Probes (Eugene, OR). Fluorescent transferrin and cholera toxin B were from Molecular Probes. Polystyrene-latex beads 100 nm in diameter, and loaded with a fluorochrome compatible with FITC fluorescence (Fluoresbrite YG microspheres), were purchased from Polysciences (Warrington, PA). Unless otherwise stated, all other reagents were from Sigma (St Louis, MO).

Cell culture

Pooled human umbilical vein endothelial cells (HUVEC) from Clonetics (San Diego, CA) were maintained in M199 medium (GibcoBRL, Grand Island, NY) supplemented with 15% fetal bovine serum (FBS), 2 mM glutamine, 15 μg/ml endothelial cell growth supplement (ECGS), 100 μg /ml heparin, 100 U/ml penicillin and 100 μg/ml streptomycin. EAhy926 cells from an endothelial-like hybrid cell line generated from HUVEC and A549 cells (Edgell et al., 1983) were cultured in DMEM medium (GibcoBRL) supplemented with 10% FBS, glutamine and antibiotics. Cultures were maintained at 37°C, 5% CO_2 and 95% relative humidity in 1% gelatin-coated tissue culture plastic. HUVEC were used between passage 4 and 5. When seeded for experiments, the cells were cultured onto 12 mm^2 gelatin-coated coverslips in 24-well plates in the absence of antibiotics and then treated with tumor necrosis factor-α (TNF-α) for at least 16 hours.

Preparation of immunobeads and immunoconjugates

Fluorescent microspheres were coated with either anti-ICAM-1, anti-PECAM-1 or control murine IgG by incubation at room temperature (RT) for 1 hour as previously described (Wiewrodt et al., 2002). The coated microspheres (immunobeads) were centrifuged to remove unbound antibodies, then resuspended in 1% bovine serum albumin-PBS and microsonicated for 20 seconds at low power. The effective immunobead diameter was determined by dynamic light scattering (DLS) using BI-90Plus particle size analyzer with BI-9000AT Digital auto-correlator (Brookhaven Instruments, Brookhaven, NY) as previously described (Wiewrodt et al., 2002). This immunobead protocol yielded uniform preparations with particle diameters ranging from 180 to 250 nm. For anti-ICAM-1 immunoconjugates, anti-ICAM-1 was biotinylated and complexed to streptavidin (90% unlabeled, 10% rhodamine labeled) in a manner equivalent to anti-PECAM-1 immunoconjugates as previously described (Wiewrodt et al., 2002). The ratio of biotinylated-ICAM-1 to streptavidin was varied to generate immunoconjugates either smaller than 500 nm or larger than 1000 nm, as determined by DLS.

Binding and uptake of anti-ICAM-1 and anti-PECAM-1 immunobeads

Confluent HUVEC or EAhy926 cells were pre-incubated overnight with 250 units of TNF-α. By flow cytometry, TNF-α treatment increased ICAM-1 expression by HUVEC and EAhy926 cells ~10-fold and had little effect on PECAM-1 expression, which is consistent with previously published results (Delisser and Albeda, 1998). The cells were then washed in serum-free medium and incubated in 1% BSA-medium containing a 1:10 dilution of either uncoated microspheres, or immunobeads coated with control murine IgG, anti-ICAM-1 or anti-PECAM-1. The cells were incubated with immunobead preparations for different time periods at 4°C or 37°C, washed in medium and fixed with 2% paraformaldehyde at RT. To distinguish between surface-bound or internalized immunobeads, nonpermeabilized fixed cells were counterstained for 30 minutes at RT with Texas Red (TxR)-conjugated goat anti-mouse IgG to produce double-labeled, yellow particles. The cells were washed in PBS, mounted onto slides with Mowiol and analyzed by fluorescence microscopy. Alexa Fluor 594-labeled cholera toxin B (FL-cholera toxin) counterstained with goat anti-cholera toxin + fluorescein rabbit anti-goat IgG was used as a control for caveolae-mediated uptake. TxR-labeled transferrin counterstained with goat anti-transferrin + fluorescein rabbit anti-goat IgG was used as a control for clathrin-mediated endocytosis.

To identify compartments containing internalized immunobeads, HUVEC monolayers were incubated with immunobeads for 1 hour at 4°C to allow surface binding, washed, then incubated at 37°C for different time periods to permit endocytosis. The cells were fixed, permeabilized and incubated with rabbit polyclonal anti-human caveolin-1, followed by incubation with goat anti-rabbit IgG conjugated to Alexa Fluor 350. Colocalization with clathrin heavy chain was done in a comparable manner, using TRITC-conjugates anti-clathrin.

For microscopy, samples mounted onto glass slides were observed using an Olympus IX70 inverted fluorescence microscope, 40× or 60× PlanApo objectives and filters optimized for fluorescent immunobeads (excitation BP460-490 nm, dichroic DM505 nm, emission BA515-

550 nm), TxR fluorescence (excitation BP530-550 nm, dichroic DM570 nm, emission BA590-800+ nm) and Alexa Fluor 450 (excitation BP360-370 nm, dichroicDM400 nm, emission BA420-460 nm) (Chroma Technology, Brattleboro, VT). Separate images for each fluorescence channel were acquired using a Hamamatsu Orca-1 CCD camera. The images were then merged and analyzed with ImagePro 3.0 imaging software (Media Cybernetics, Silver Spring, MD) as previously described (Wiewrodt et al., 2002). For quantitation, merged images of cells labeled with immunobeads were scored automatically for total green fluorescent particles and noninternalized immunobeads (double-labeled yellow particles). Uptake was calculated as the percentage of internalized immunobeads with respect to the total number of cell-associated immunobeads. Statistical significance was determined by Student's *t* test.

Mechanisms of ICAM-1- and PECAM-1-mediated uptake

Mammalian pcDNA3 expression vectors encoding for 6-His-tagged versions of human dynamin-2 [wild-type and dominant-negative forms (K44A), (PH*)] were gifts from Drs S. Schmid (Scripps Research Institute, La Jolla, CA) (Altschuler et al., 1998) and M. Lemmon (U Penn School of Medicine, Philadelphia, PA) (Lee et al., 1999). EAhy926 endothelial cells were transfected using Lipofectin (GibcoBRL) complexed to 1.5 μg DNA/dish encoding either dynamin-2, dynamin-2(K44A) or dynamin-2(PH*). Each construct includes a 6-His amino terminus tag to distinguish it from endogenous dynamin-2. Twelve hours after transfection, the cells were stimulated with TNF-α, incubated for 36 hours and then anti-ICAM-1 or anti-PECAM-1 uptake was determined by double labeling as described above. Following labeling of surface-bound material, the cells were permeabilized with 0.2% Triton X-100 and then immunostained using 5 μg/ml rabbit anti-6-His-Tag and goat anti-rabbit IgG conjugated to Alexa Fluor 350 to identify cells expressing recombinant dynamin-2.

For studies using pharmacological inhibitors, TNF-α-stimulated HUVEC or EAhy926 were pre-incubated for 30 minutes at 37°C in the presence of one of the following agents: 50 μM monodansyl-cadaverine (MDC), 1 μg/ml filipin, 50 μM genistein, 3 mM amiloride, 25 μM monensin, 0.5 mM cytochalasin D, 0.1 μM latrunculin A, 20 μM nocodazole, 5 μM bisindolyl-maleimide-1 (BIM-1), 10 μM 1-(5-isoquiniline sulphonyl)-2-methylpiperazine (H7), 0.1 μM phorbol 12-myristate 13-acetate (PMA), 10 μM radicicol, 10 μM Y-27346 or 0.5 μM wortmannin (Barreiro et al., 2002; Fujimoto et al., 2000; Parton et al., 1994; Racoosin and Swanson, 1989; Sahai and Marshall, 2002; Schlegel et al., 1982; Schnitzer et al., 1994; Swanson, 1989; Torgersen et al., 2001; Watanabe et al., 2001; West et al., 1989). Molecular targets for selected inhibitors are shown in Fig. 10. The concentration of each agent was selected using literature values and was optimized qualitatively by fluorescence microscopy (not shown). Also, we examined the effectiveness of each agent using suitable controls (e.g. Fig. 4). Potassium depletion was done by pre-incubating the cells for 15 minutes in potassium depletion buffer (0.14 M NaCl, 2 mM $CaCl_2$, 1 mg/ml glucose, 20 mM HEPES, pH 7.4) diluted 1:1 with water to make it hypotonic (Koval et al., 1998). After treatment, the cells were incubated with immunobeads, cholera toxin or transferrin at 37°C, in the presence of K^+-depletion buffer or the given inhibitors, and then fixed and double labeled for surface-bound material as described above.

Results

Monomeric antibodies to PECAM-1 are poorly internalized by endothelial cells (Muzykantov et al., 1999; Wiewrodt et al., 2002). Multivalent anti-PECAM-1 conjugates with a diameter of 100-300 nm are readily internalized, but the efficiency of internalization decreases with increasing conjugate size (Wiewrodt et al., 2002). To test whether this is the case for anti-ICAM-1 conjugates, we examined the internalization of anti-ICAM-1 conjugates in two different size ranges by TNF-α-stimulated HUVEC (Fig. 1A,B). Consistent with our previous results using anti-PECAM-1 conjugates, we found that anti-ICAM-1 conjugates with a diameter less than 500 nm were

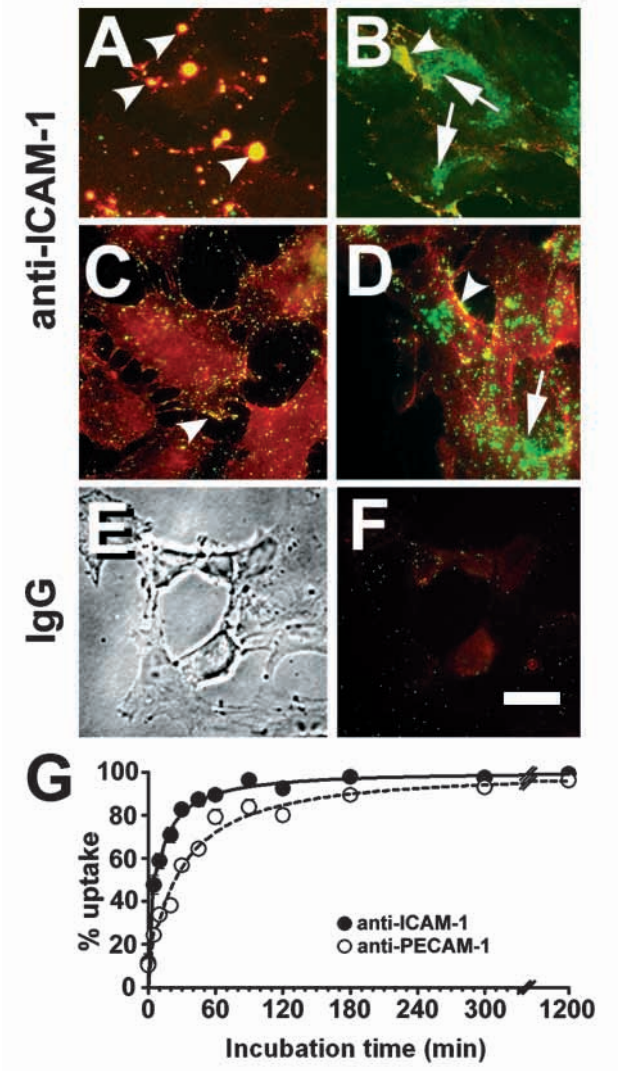

Fig. 1. Small ICAM-1 immunoconjugates are internalized by HUVEC. HUVEC were treated with 250 U TNF-α for 24 hours. Confluent monolayers were incubated at either 4°C (c) or 37°C (A,C-F) in the presence of either large (A; >1000 nm diameter), small (b; <500 nm diameter) biotin-anti-ICAM-1/streptavidin conjugates, anti-ICAM-1 immunobeads (C,D) or beads previously coated with control murine IgG (E,F). The cells were subsequently washed, fixed and counterstained with fluorescent goat anti-mouse IgG. Merged images corresponding to representative samples were pseudocolored to show single-labeled, internalized immunoconjugates/immunobeads as green (arrows) and double-labeled immunoconjugates/immunobeads on the cell surface as yellow (arrowheads). The phase-contrast image shown in e corresponds to the fluorescence image shown in F. Bar, 10 μm. (G) Uptake of anti-ICAM-1 (●) and anti-PECAM-1 (○) immunobeads by TNF-α-activated HUVEC was determined for different incubation times as the mean percentage of internalized (single labeled) immunobeads per cell. Error bars corresponding to s.d. were smaller than the size of the symbols used for the graph.

internalized by HUVEC, whereas conjugates with diameter greater than 1000 nm showed little, if any, internalization. Because antibody conjugates show a broad distribution of particle sizes (Wiewrodt et al., 2002), we performed subsequent experiments using anti-ICAM-1 and anti-PECAM-1 immunobeads, which have a more uniform diameter in the size range that allows internalization (Wiewrodt et al., 2002). Anti-ICAM-1 immunobeads were internalized by HUVEC when incubated at 37 °C but not at 4°C (Fig. 1C,D). Similar results were obtained using anti-PECAM-1 beads (S.M., R.W. and A.T. et al., unpublished). Following internalization, there was further clustering of conjugates and immunobeads, which was probably due to endosome fusion events that occurred as the particles were transported along the endocytic pathway.

On average, ~125 immunobeads/cell were internalized after a 1 hour incubation at 37°C. Fig. 1G shows that uptake of anti-ICAM-1 immunobeads was more rapid (~10 minutes half time for uptake) than that of anti-PECAM-1 immunobeads (~20 minutes half time for uptake). Similar results were obtained for anti-ICAM-1 and anti-PECAM-1 immunobeads internalized by naïve HUVEC, indicating that TNF-α had little effect on the mechanism of internalization. This also suggests that the mechanism for internalization is not sensitive to the surface density of ICAM-1, as virtually all of the anti-ICAM-1 immunobeads were internalized after 30 minutes at 37°C, despite the difference in binding in the absence (42±15 beads/cell) or presence of TNF-α (165±54 beads/cell). Also, as found for anti-PECAM-1, monomeric anti-ICAM-1 was not internalized (S.M., R.W. and A.T. et al., unpublished).

Because dynamin-2 is frequently involved in vesicle-mediated internalization and phagocytosis (Altschuler et al., 1998; Gold et al., 1999; Henley et al., 1998; Lee et al., 1999), we examined the role for dynamin-2 in uptake of anti-ICAM-1 immunobeads. Given the low transfection rate of HUVEC, we used the endothelial-like cell line, EAhy926, which showed a 40% transfection efficiency using Lipofectin. EAhy926 cells internalized anti-ICAM-1 immunobeads in a manner comparable to HUVEC (Fig. 2). These cells were transiently transfected to express amino-terminal 6-His-tagged forms of either wild-type or dominant-negative dynamin-2 (K44A or PH*). Expression of recombinant proteins was identified by immunofluorescence, using an antibody that recognizes the 6-His epitope (Fig. 2). Cells transfected with wild-type dynamin-2 showed no effect on the uptake of anti-ICAM-1 immunobeads compared with control cells. By contrast, cells expressing ether dynamin-2(K44A) or dynamin-2(PH*) showed less anti-ICAM-1 immunobead uptake than control cells, suggesting that uptake of these immunobeads required dynamin-2 (Fig. 2). This was not due to a net decrease in immunobead binding, which was equivalent for nontransfected EAhy926 cells (23±3 beads/cell) and EAhy926 cells expressing wild-type (24±16 beads/cell) or mutant dynamin-2 [25±4 beads/cell (PH*), 14±5 beads/cell (K44A)].

We also found that the dominant-negative dynamin-2 constructs inhibited the uptake of Alexa Fluor 594-conjugated cholera toxin (FL-cholera toxin, S.M., R.W. and A.T. et al., unpublished) that is internalized by caveolae-mediated endocytosis (Schnitzer et al., 1994). However, few, if any, anti-ICAM-1 immunobeads colocalized with caveolin-1-positive structures, regardless of whether the immunobeads were bound to the plasma membrane or internalized by HUVEC (Fig. 3).

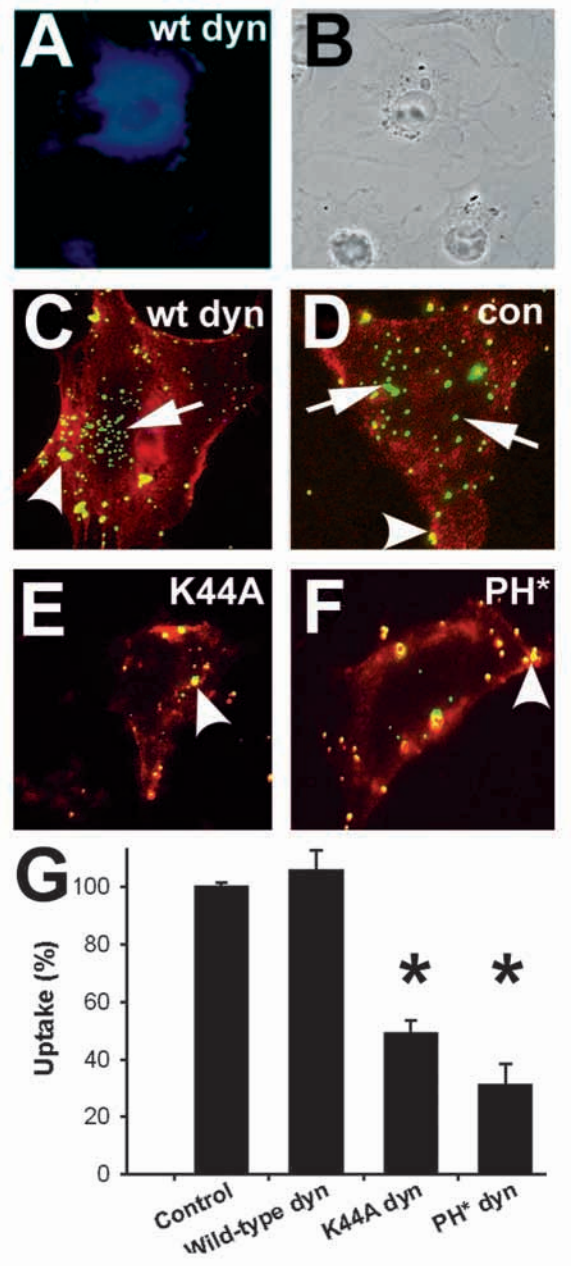

Fig. 2. Anti-ICAM-1 immunobead uptake is inhibited by dominant-negative dynamin constructs. EAhy926 cells were transfected with 1.5 μg of DNA encoding either wild-type (A-C) or dominant-negative (K44A; e, PH*; f) dynamin-2. Nontransfected cells are shown in (D). Twelve hours post-transfection, cells were stimulated with TNF-α for 36 hours and then incubated for 2 hours at 37°C with anti-ICAM-1 immunobeads. The cells were then washed, fixed and surface-bound particles were counterstained with TxR goat anti-mouse IgG. The cells were then permeabilized and stained with rabbit anti-6-His antibody followed by Alexa Fluor 350 goat anti-rabbit IgG to identify transfected cells expressing dynamin (A). The corresponding phase-contrast image is shown in (B). Merged images corresponding to representative samples of transfected (C,E,F) or control (D) cells are shown, where single-labeled, internalized immunobeads are green (arrows) and double-labeled immunobeads on the cell surface are yellow (arrowheads). Blue fluorescence of transfected cells is omitted in panels (C,E,F) to enable better visualization of red and green fluorescence. (G) The percentage of immunobead uptake was calculated as described as mean±s.d. *P<0.05.

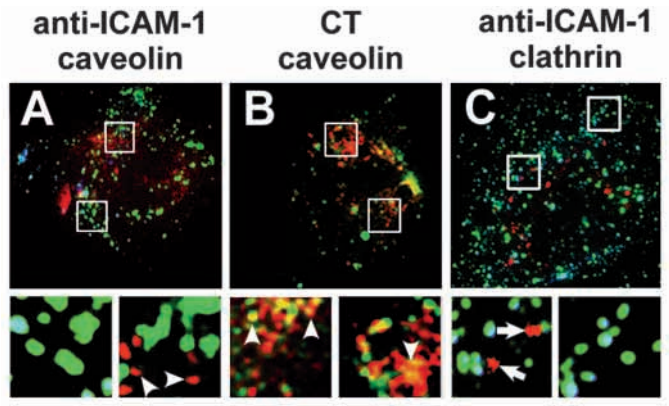

Fig. 3. Anti-ICAM-1 immunobeads do not colocalize with caveolin or clathrin. TNF-α-stimulated HUVEC were incubated with control anti-ICAM-1 immunobeads (A,C) or Alexa 594-conjugated cholera toxin B subunit (B) for 15 minutes at 37°C. The cells were then washed and fixed, and surface-bound material was counterstained with TxR goat anti-mouse IgG (A,C) or goat anti-cholera toxin followed by fluorescein rabbit anti-goat IgG (B). After permeabilization, the cells were then labeled with rabbit anti-human caveolin-followed by Alexa 350-conjugated goat anti-rabbit IgG (A,B) or TRITC-conjugated anti-clathrin heavy chain (C). Insets show images magnified twofold. The image color channels were selected to facilitate the comparison between panels in the figure, and they are: green, internalized immunobeads or cholera toxin; blue, surface-bound immunobeads or cholera toxin; red, caveolin-1 (arrowheads) or clathrin (arrows). There was little, if any, colocalization of anti-ICAM-1 immunobeads with caveolin-1 or clathrin, as evidenced by the lack of yellow labeling in A and C and areas showing internalized immunobeads with little caveolin-1 or clathrin nearby (see insets).

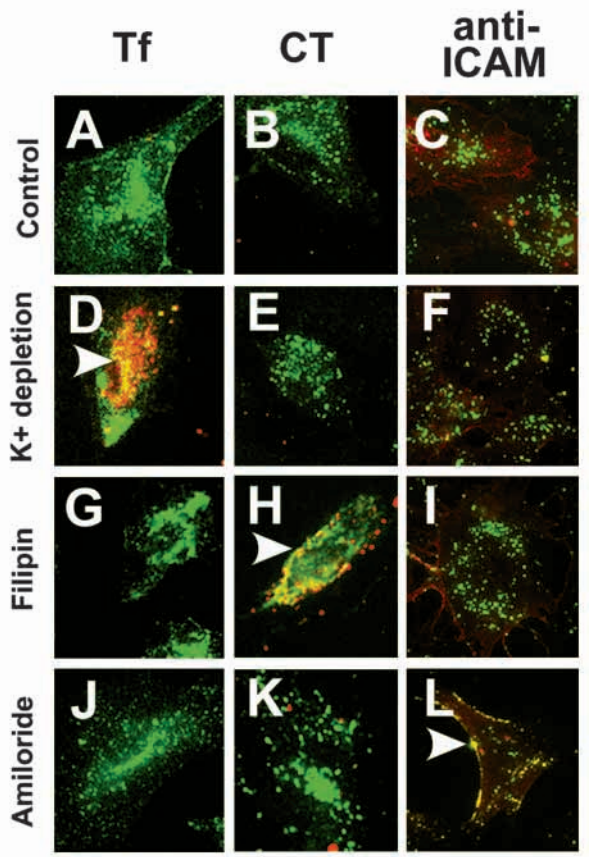

Fig. 4. Anti-ICAM-1 conjugates are not internalized by clathrin or caveolae-mediated endocytosis. TNF-α-activated HUVEC were untreated (A-C), potassium-depleted (D-F), or treated for 30 minutes at 37ºC with 1 μg/ml filipin (G-I), or 3 mM amiloride (J-L). The cells were incubated in the presence or absence of inhibitors for 1 hour at 37°C with fluorescent transferrin (Tf: A,D,G,J), fluorescent cholera toxin (CT: B,E,H,K) or anti-ICAM-1 immunobeads (C,F,I,L), then fixed and counterstained to double-label surface-bound material (yellow, arrowheads). As shown, potassium depletion specifically inhibited transferrin uptake by clathrin-mediated endocytosis (D), filipin specifically inhibited caveolar uptake of cholera toxin (H) and amiloride specifically inhibited uptake of anti-ICAM-1 immunobeads (L).

By contrast, FL-cholera toxin showed extensive colocalization with caveolin, which is consistent with previously published reports (Puri et al., 2001). Newly internalized anti-ICAM-1 immunobeads also did not colocalize with clathrin. In fact, there was a low level of clathrin immunofluorescence shown by HUVEC, consistent with a less-dominant role for clathrin-coated pits in endocytosis than caveolae-mediated pathways in endothelial cells (Schubert et al., 2001). Thus, despite being a dynamin-dependent process, anti-ICAM-1 conjugate uptake by endothelial cells was unlikely to be through caveolae- or clathrin-coated vesicles.

We therefore used a series of pharmacological inhibitors to further characterize internalization of anti-ICAM-1 and anti-PECAM-1 conjugates by HUVEC. The specificity of different inhibitors was confirmed using fluorescent transferrin and cholera toxin as controls for clathrin-mediated and caveolar endocytosis, respectively (Fig. 4). As shown in Fig. 5, inhibitors of clathrin-mediated transferrin endocytosis (MDC, potassium depletion) did not inhibit the uptake of anti-ICAM-1 or anti-PECAM-1 immunobeads. Furthermore, inhibitors of caveolae-dependent cholera toxin uptake (filipin, genestein) were not effective at inhibiting anti-ICAM-1 or anti-PECAM-1 immunobead internalization. Because uptake of anti-ICAM-1 and anti-PECAM-1 immunobeads appeared to be through a unique internalization pathway, we examined the effect of other inhibitors on immunobead endocytosis. Previous work has indicated that amiloride, an inhibitor of the sodium/proton pump, can inhibit macropinocytosis by dendritic cells (West et al., 1989). Amiloride had little effect on internalization of FL-cholera toxin or transferrin, suggesting that it did not inhibit caveolae- or clathrin-mediated endocytosis (Fig. 4). However, amiloride inhibited uptake of anti-ICAM-1 and anti-PECAM-1 immunobeads by HUVEC (55±15% and 60±9%, respectively) and by EAhy926 cells (34±9% and 24±3% inhibition, respectively. Anti-ICAM-1 immunobead binding was equivalent for control (125±21 beads/cell) and amiloride-treated HUVEC (154±37 beads/cell), suggesting that amiloride did not decrease ICAM-1 surface expression. TNF-α stimulation was not required, given that amiloride inhibited anti-PECAM-1 immunobead uptake by naïve HUVEC by 50.5±6.2%. Also, anti-ICAM-1 immunobead uptake by amiloride-treated HUVEC remained inhibited during a 3 hour (43.8±2.9%) and 5 hour incubation (50.6±5.2%), suggesting that amiloride altered the extent of immunobead uptake, rather than uptake kinetics. Furthermore, this was not likely to be due to an effect on ion homeostasis, given that the ionophore

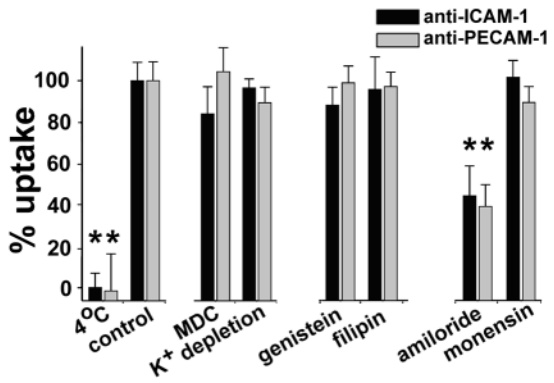

Fig. 5. Effect of endocytosis inhibitors on anti-ICAM-1 and anti-PECAM-1 uptake. Uptake of anti-ICAM-1 and anti-PECAM-1 immunobeads was quantified as mean±s.d. by fluorescence microscopy using control cells, potassium-depleted cells or cells pretreated for 30 minutes at 37°C before incubation with immunobeads with either 50 μM MDC, 50 μM genistein, 1 μg/ml filipin, 3 mM amiloride or 25 μM monensin. Cells incubated with anti-ICAM-1 or anti-PECAM-1 immunobeads at 4°C are controls for no internalization. **P*<0.05.

monensin had little, if any, effect on anti-ICAM-1 and anti-PECAM-1 immunobead uptake (Fig. 5).

Because protein kinase C (PKC) has been reported to play a pivotal role in macropinocytosis and phagocytosis by macrophages (Araki et al., 1996; Larsen et al., 2000; Swanson, 1989), we tested the effect of PKC inhibitors on immunobead internalization by HUVEC. As shown in Fig. 6, the PKC inhibitors BIM-1 and H-7 inhibited immunobead uptake by ~30% and ~60%, respectively. H-7 treatment also inhibited the uptake of anti-ICAM-1 and anti-PECAM-1 by EAhy926 cells by 55±11% and 48±7%, respectively. HUVEC pretreated with 0.1 μM PMA for 30 minutes (conditions that stimulate PKC activity) showed a high level of anti-ICAM-1 and anti-PECAM-1 internalization (>95%), and the total level of immunobead uptake by HUVEC was stimulated nearly twofold. Anti-ICAM-1 immunobead binding was equivalent for control (125±21 beads/cell) and BIM-1-treated HUVEC (140±7 beads/cell), suggesting that BIM-1 did not decrease ICAM-1 surface expression. Stimulation by TNF-α was not required, since inhibiting PK-C activity also inhibited uptake of anti-PECAM-1 immunobeads by naïve HUVEC (47.5±9.8%) and uptake of anti-PECAM-1 immunobeads by naïve HUVEC was enhanced 1.3-fold by PMA. Also, anti-ICAM-1 immunobead uptake by BIM-1-treated HUVEC remained inhibited during a 3 hour (39.6±4.2%) and 5 hour incubation (42.9±5.2%), suggesting that BIM-1 altered the extent of immunobead uptake, rather than uptake kinetics. Taken together, these results are consistent with internalization of anti-ICAM-1 and anti-PECAM-1 immunobeads by a PKC-dependent pathway. However, since H-7 may also interfere with actin-based contractility (Volberg et al., 1994), this effect may also contribute to the inhibition of uptake.

In fact, the formation of F actin stress fibers is frequently associated with ICAM-1 crosslinking (Thompson et al., 2002; Wang and Doerschuk, 2002). Therefore, we examined the effect of anti-ICAM-1 immunobeads on the formation of actin stress fibers by HUVEC. As shown in Fig. 7, stress fibers were rapidly

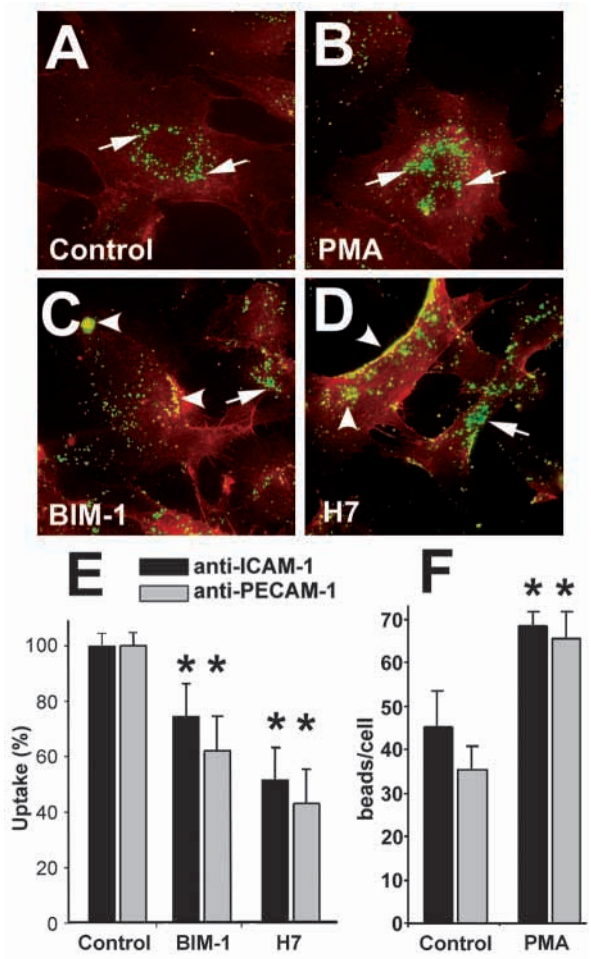

Fig. 6. Uptake of anti-ICAM-1 or anti-PECAM-1 immunobeads is PKC-mediated. TNF-α-activated HUVEC were treated for 30 minutes with vehicle alone (A), 0.1 μM PMA (B), 0.1 μM BIM-1 (C) or 10 μM H-7 (D), then incubated with anti-ICAM-1 or anti-PECAM-1 immunobeads for 1 hour at 37°C, then fixed and immunostained to double-label surface-bound material (yellow, arrowheads). Arrows denote internalized immunobeads. Uptake of anti-ICAM-1 and anti-PECAM-1 immunobeads was quantified as mean±s.d. by fluorescence microscopy for these treatments, expressed as a percentage of immunobead uptake for the PKC inhibitors (E). For PMA, this is expressed as the total number of internalized particles per cell (F), as the percent internalization was equivalent for control and PMA stimulated cells. **P*<0.05.

induced by anti-ICAM-1 immunobead binding. Immunobeads appeared to align along actin stress fibers before internalization; this is shown most prominently by the blue labeled immunobeads in Fig. 7C,D. Vesicles containing internalized immunobeads continued to be associated with stress fibers after internalization and remained associated with actin during a 3 hour incubation. Few, if any, anti-ICAM-1 immunobeads induced formation of an actin coat (phagocytic cup) at the site of internalization, which is a hallmark of phagocytosis and macropinocytosis (Grimmer et al., 2002; Lee and Knecht, 2002). Note that this is probably not a problem with the detection of actin coats, as a previous study found that ~20% of 0.2 μm beads internalized by Fc receptors in macrophages were associated with actin coats (Koval et al., 1998).

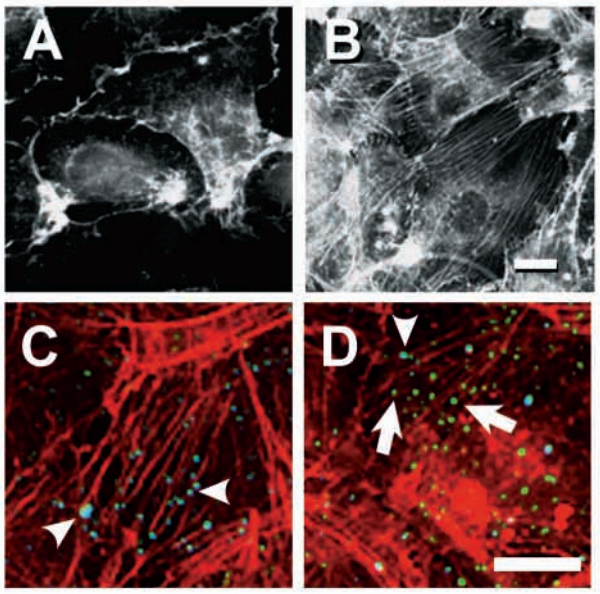

Fig. 7. Internalized anti-ICAM-1 immunobeads associate with the actin cytoskeleton. (A,b) HUVEC incubated in either the absence (A) or presence (B) of anti-ICAM-1 immunobeads for 15 minutes were fixed and then treated with rhodamine phalloidin to label filamentous actin. Note the stimulation of actin stress fibers by anti-ICAM-1 immunobeads. Bar, 10 μm. (C,D) HUVEC were incubated with anti-ICAM-1 immunobeads for 15 (C) or 30 (D) minutes, fixed, then immunostained to double-label surface-bound material (blue, arrowheads). Arrows denote internalized immunobeads in vesicles associated with stress fibers. Bar, 10 μm.

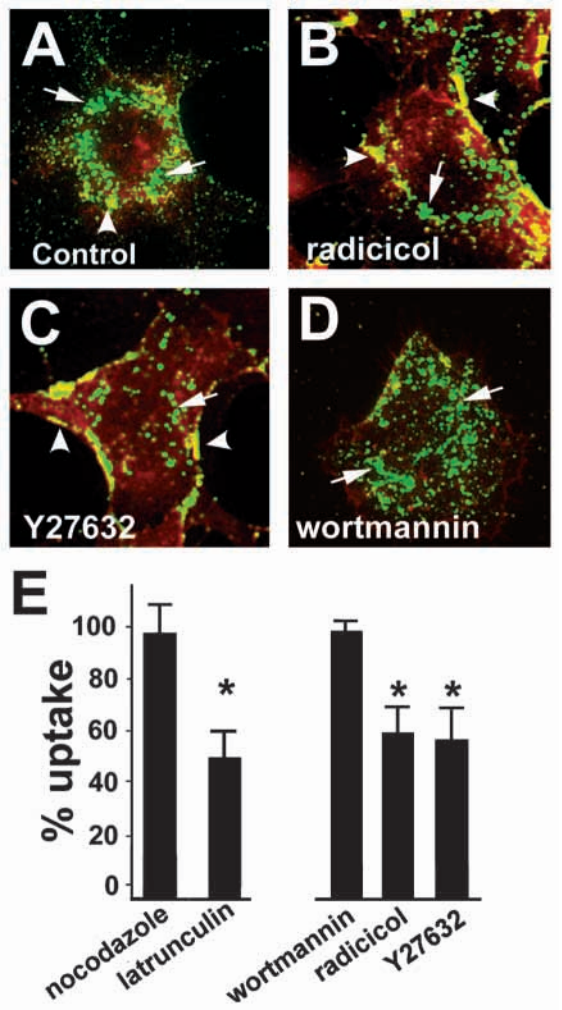

Fig. 8. Uptake of anti-ICAM-1 immunobeads requires actin regulatory proteins. TNF-α activated HUVEC were treated for 30 minutes with vehicle alone (A), 10 μM latrunculin A, 20 μM nocodazole, 10 μM radicicol (B), 10 μM Y-27632 (C) or 0.5 μM wortmannin (D), then incubated with anti-ICAM-1 immunobeads for 1 hour at 37°C, then fixed and immunostained to double-label surface-bound material (yellow, arrowheads). Arrows denote internalized immunobeads. Uptake of anti-ICAM-1 immunobeads was quantified as mean±s.d. by fluorescence microscopy for these treatments, expressed as a percentage of immunobead uptake. Uptake required both Src kinase activity and ROCK activity, since it was inhibited by radicicol and Y27632, but did not appear to require PI-3 kinase activity, as wortmannin had no measurable effect on uptake. **P*<0.05.

Given the dramatic association of anti-ICAM-1 immunobeads with actin in HUVEC, we also examined the cytoskeletal requirements for the uptake of anti-ICAM-1 and anti-PECAM-1 immunobeads. In contrast to macropinocytosis by macrophages (Racoosin and Swanson, 1992), microtubules were not required for the internalization of anti-ICAM-1 immunobeads by HUVEC, since internalization was not inhibited by nocodazole (Fig. 8). Also, nocodazole did not significantly inhibit the uptake of anti-PECAM-1 immunobeads (12±9% inhibition). Cytochalasin D, which caps short actin filaments, had little effect on the uptake of anti-ICAM-1 immunobeads (18±7% inhibition) or anti-PECAM-1 immunobeads (8±8% inhibition). However, the more effective actin depolymerizing agent, latrunculin, inhibited anti-ICAM-1 immunobead uptake (Fig. 8) and uptake of anti-PECAM-1 immunobeads (69±15% inhibition).

We also examined inhibitors that affect kinases known to play a role in regulating actin organization. In contrast to macropinocytosis by phagocytes (Araki et al., 1996; West et al., 2000), wortmanin had little, if any, effect on uptake of anti-ICAM-1 immunobeads by HUVEC, suggesting that PI3-kinases were not involved in immunobead uptake. However, as shown in Fig. 8, uptake of anti-ICAM-1 immunobeads was inhibited by the Src kinase inhibitor radicicol and the ROCK inhibitor Y27632, consistent with the notion that both the PKC pathway and Rho pathway regulate actin cytoskeletal rearrangements required for internalizaton of clustered ICAM-1. Four inhibitors of anti-ICAM-1 immunobead internalization – latrunculin, amiloride, radicicol and Y27632 – all inhibit the formation of actin stress fibers induced by anti-ICAM-1 immunobead binding (Fig. 9), underscoring the correlation of uptake by HUVEC with actin mobilization.

Discussion

In this study, we found that endothelial cells internalize clustered ICAM-1 and clustered PECAM-1 by a novel endocytic pathway (Table 1). CAM-mediated endocytosis was distinct from caveolae-mediated uptake (McIntosh et al., 2002; Minshall et al., 2000; Predescu et al., 1998) as it was not inhibited by genestein or filipin and the bound conjugates did

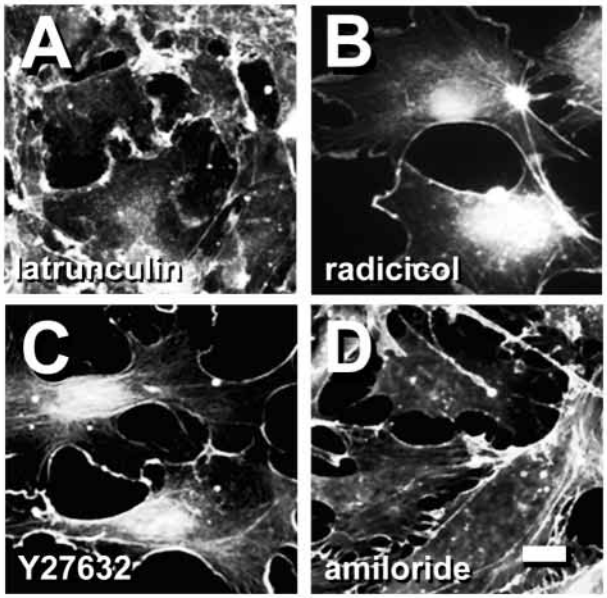

Fig. 9. Agents that inhibit anti-ICAM-1 immunobead uptake disrupt actin rearrangements induced by immunobeads. HUVEC were pretreated with 10 μM latrunculin A (A), 10 μM radicicol (B), 10 μM Y-27632 (C) or 3 mM amiloride (D), incubated with anti-ICAM-1 immunobeads for 15 minutes then fixed and stained for filamentous actin using rhodamine phalloidin. Each of these agents that inhibit uptake of anti-ICAM-1 immunobeads also inhibited actin stress-fiber formation. Bar, 10 μm.

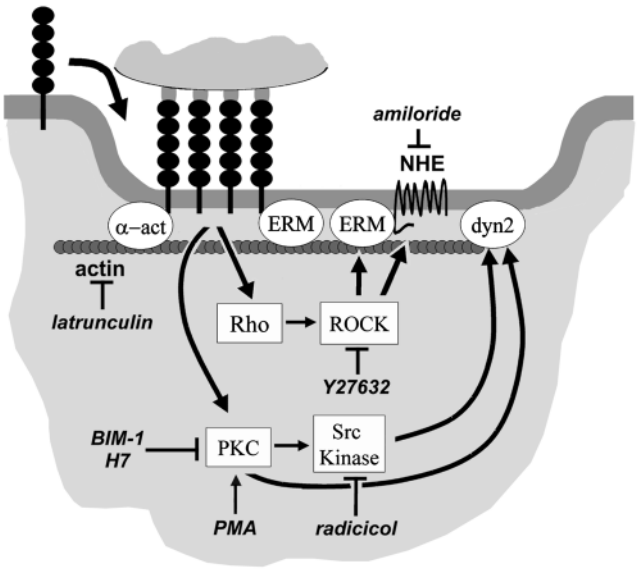

Fig. 10. Model for uptake mediated by cell adhesion molecules. The model shown is for signaling pathways stimulated when monomeric ICAM-1 or anti-PECAM-1 are clustered by binding to immunoconjugates. Pharmacological inhibitors and activators are indicated by italics. Cell adhesion molecules have the capacity to bind proteins that mediate direct interactions with the actin cytoskeleton, such as α-actinin (α-act) and ERM proteins. On the basis of our inhibitor data and results from the literature, we propose that clustering of ICAM-1 or PECAM-1 can also stimulate PKC, Src kinase and ROCK signal transduction pathways. This could help regulate the recruitment of other cofactors, such as dynamin-2 (dyn2), to the plasma membrane. Also, ERM proteins and NHE transporters are downstream targets for phosphorylation by the Rho/ROCK pathway, which might further serve to recruit actin to sites of immunoconjugate uptake in response to ICAM-1 or PECAM-1 clustering.

not colocalize with caveolin. Also, uptake of anti-ICAM-1 and anti-PECAM-1 conjugates was distinct from clathrin-mediated endocytosis, because it was not inhibited by potassium depletion or MDC and the conjugates did not colocalize with clathrin (Hansen et al., 1993; Schlegel et al., 1982). Whether CAM-mediated endocytosis is specific for endothelial cells remains to be determined, although PECAM-1 transfected REN mesothelioma cells show a similar endocytic pathway (Wiewrodt et al., 2002).

On the basis of amiloride sensitivity and PKC dependence, internalization of clustered anti-ICAM-1 and anti-PECAM-1 seemed to be related to macropinocytosis (Lamaze and Schmid, 1995; Nichols and Lippincott-Schwartz, 2001; Orth et al., 2002; Swanson and Watts, 1995), a pathway that is not typically associated with endothelial cells. Nonetheless, CAM-mediated endocytosis was distinct from 'classical' macropinocytosis, on the basis of several criteria (Table 1). For example, in contrast to the dynamin-2 requirement we observed for uptake of anti-ICAM-1 immunobeads by EAhy926 endothelial cells, the K44A dominant-negative dynamin-2 did not inhibit macropinocytosis by fibroblasts (Orth et al., 2002). Although dynamin is required for endocytosis (Altschuler et al., 1998; Henley et al., 1998; Lee et al., 1999) and phagocytosis (Gold et al., 1999), CAM-mediated endocytosis differed in other ways from these processes. For instance, anti-ICAM-1 immunobeads did not colocalize with either clathrin or caveolin (Fig. 4). Also, uptake of anti-ICAM-1 immunobeads did not require PI3K activity, which is needed for phagocytosis (Araki et al., 1996; Cox et al., 1999), as well as macropinocytosis (West et al., 2000).

The uptake of anti-ICAM-1 and anti-PECAM-1 conjugates required clustering of cell adhesion molecules (Muzykantov et al., 1999; Wiewrodt et al., 2002). ICAM-1 clustering has been found to stimulate multiple intracellular signaling pathways (Adamson et al., 1999; Etienne et al., 1998), including a PKC signaling pathway that results in the phosphorylation of cytoskeletal and focal adhesion proteins, thereby enabling actin filament rearrangement (Etienne-Manneville et al., 2000). Consistent with this, anti-ICAM immunobeads induced actin stress fiber formation and were associated with stress fibers before internalization (Fig. 7). Both Src kinase and ROCK activity are required for CAM-mediated endocytosis and these inhibitors also inhibited stress fiber formation induced by anti-ICAM-1 immunobeads (Fig. 9). ROCK activity also enables remodeling of F-actin attached to adherence junctions and controls their stability (Sahai and Marshall, 2002). This also provides a potential link between ICAM-1 or PECAM-1 clustering, Src kinase, PKC and dynamin-2 (Fig. 10), as dynamins are downstream targets for Src kinase (Ahn et al., 2002) and PKC (Powell et al., 2000).

Dynamin, via interactions with endophilin and profilin, helps recruit actin to sites of endocytic activity (Farsad et al., 2001; Witke et al., 1998). Proteins in the ezrin-radixin-moesin (ERM) family are also good candidates to link internalization

Table 1. Comparison of CAM-mediated endocytosis with phagocytosis and macropinocytosis

	CR-mediated phagocytosis	FcR-mediated phagocytosis	Macropinocytosis	CAM-mediated endocytosis	Distinct from‡
Internalize particles >1 μm	Yes	Yes	Yes	No	CFM
Receptor clustering	+*	+	–	+	M
Dynamin-2	+	+	–	+	M
NHE	–	–	+	+	CF
PKC	+	+	+	+	n
Actin	+	+	+	+	n
Actin cup	+	+	+	–	CFM
Microtubules	+	–	+	–	CM
Src kinase	–	+	+	+	C
PI-3 kinase	+	+	+	–	CFM
Rho kinase	+	–	?	+	F

Table adapted from Caron and Hall (Caron and Hall, 2001) and expanded. For references to specific elements, see text.

*+, required for uptake; –, not required for uptake; ?, unknown.

‡C, distinct from complement receptor (CR)-mediated phagocytosis; F, distinct from FcR-mediated phagocytosis; M, distinct from macropinocytosis; n, none, common to all listed pathways.

of ICAM-1 and PECAM-1 to the actin cytoskeleton (Bretscher et al., 1997; Cao et al., 1999). For instance, ezrin binds directly to the C-terminus of ICAM-1 (Heiska et al., 1998). Another actin binding protein, α-actinin, has also been shown to bind to the C-terminus of ICAM-1 (Carpen et al., 1992). Perhaps signaling induced by ICAM-1 or PECAM-1 clustering can indirectly recruit ERM proteins to the plasma membrane. For instance, phosphorylation of ERM proteins by a ROCK-dependent pathway can help recruit them to the plasma membrane (Hirao et al., 1996). Intriguingly, ROCK activity has been associated with complement receptor-mediated phagocytosis, but is not required for Fc receptor-mediated endocytosis (Olazabal et al., 2002). ROCK has also been shown to phosphorylate sodium proton exchangers (NHE) to enhance binding of ERM proteins (Denker et al., 2000). Both processes might correspond to the ROCK requirement for uptake of clustered ICAM-1 or PECAM-1 (Fig. 10). This is further suggested by the ability of amiloride to inhibit uptake of clustered ICAM-1 and PECAM-1, since amiloride can disrupt the association of ERM proteins with NHE, an effect that is independent of ion channel activity (Denker et al., 2000; Putney et al., 2002).

Another major distinction from macropinocytosis and phagocytosis is that uptake of anti-ICAM-1 and anti-PECAM-1 conjugates larger than 500 nm in diameter was poor (Fig. 1) (Wiewrodt et al., 2002). Also, anti-ICAM-1 immunobeads smaller than 500 nm diameter did not induce the formation of an actin cup or coat (Fig. 7), which is typically induced by larger particles internalized by phagocytosis (Koval et al., 1998), suggesting that formation of an actin coat is crucial for internalization of larger particles. Although the mechanisms that cells use to control the size threshold for internalization is not known at present, given that ICAM-1 and PECAM-1 primarily regulate cell–cell contacts, a small size threshold for internalization may be a means by which endothelial cells avoid engulfing other cells.

Consistent with a size threshold for ICAM-1-mediated internalization, an ICAM-1 enriched structure is formed at the contact site between lymphocytes and HUVEC, where the endothelial cell appears to partially engulf the lymphocyte (Barreiro et al., 2002). Furthermore, the lymphocyte-endothelial cell docking structure requires ROCK activity, but not phosphatidylinositol 3-kinase (PI-3 kinase) (Barreiro et al., 2002), comparable to our observations for anti-ICAM-1 and anti-PECAM-1 immunobeads (Fig. 9). Whether plasma membrane internalization is part of the mechanism required to maintain this docking structure is not known at present. One possibility is that CAM-mediated endocytosis might help to remodel cell–cell junctions as leukocytes migrate along endothelial cells. If so, this might be analogous to the turnover of gap junctions, which is mediated by the engulfment of cell–cell junctions sites to create endocytic vesicles in the 200-500 nm diameter size range (Gaietta et al., 2002; Jordan et al., 2001).

The size threshold for internalization of clustered ICAM-1 and PECAM-1 might also enable endothelial cells to distinguish small apoptotic fragments from intact cells bound to the endothelial cell surface, such as other endothelial or blood cells (Barreiro et al., 2002; DeLisser and Albelda, 1998; Johnson-Leger et al., 2000; Worthylake and Burridge, 2001). The notion that endothelial cells could also scavenge apoptotic fragments via a pathway comparable to CAM-mediated endocytosis is appealing (Brown et al., 2002; Treutiger et al., 1997); however, whether this is the case remains to be determined.

Understanding the mechanisms that regulate uptake of anti-ICAM-1 and anti-PECAM-1 conjugates will probably help to extend the utility of these agents as the basis for endothelium-specific drug-targeting vehicles (Li et al., 2000; Muzykantov et al., 1999; Scherpereel et al., 2002; Scherpereel et al., 2001; Wiewrodt et al., 2002). For instance, inhibitors of conjugate uptake might help to increase their stability by reducing the extent of delivery to lysosomes and other degradative compartments. Animal studies combining the agents used in this work with the administration of pharmacologically active, enzyme-carrying anti-ICAM or anti-PECAM conjugates will be used to determine the feasibility of this approach.

We thank B. Daugherty for a critical reading of the manuscript. S.M. is supported by a fellowship from Fundación Ramón Areces (Spain). R.W. is a postdoctoral fellow of the Mildred Scheel Stiftung fur Krebsforschung der Deutschen Krebshilfe e.V. (D/98/02288). Supported by an American Heart Association grant-in-aid 9950389N (M.K.) National Institutes of Health SCOR in Acute Lung Injury, HL60290, Project 4, (V.R.M., S.M.A.); grants HL/GM 71175-01

(V.R.M.), GM61012 (M.K.) and P01 HL019737-26, Project 3 (M.K.) and Department of Defense Grant PR 012262 (V.R.M.).

References

Adamson, P., Etienne, S., Couraud, P. O., Calder, V. and Greenwood, J. (1999). Lymphocyte migration through brain endothelial cell monolayers involves signaling through endothelial ICAM-1 via a rho-dependent pathway. *J. Immunol.* **162**, 2964-2973.

Ahn, S., Kim, J., Lucaveche, C. L., Reedy, M. C., Luttrell, L. M., Lefkowitz, R. J. and Daaka, Y. (2002). Src-dependent tyrosine phosphorylation regulates dynamin self-assembly and ligand-induced endocytosis of the epidermal growth factor receptor. *J. Biol. Chem.* **277**, 26642-26651.

Altschuler, Y., Barbas, S. M., Terlecky, L. J., Tang, K., Hardy, S., Mostov, K. E. and Schmid, S. L. (1998). Redundant and distinct functions for dynamin-1 and dynamin-2 isoforms. *J. Cell Biol.* **143**, 1871-1881.

Araki, N., Johnson, M. T. and Swanson, J. A. (1996). A role for phosphoinositide 3-kinase in the completion of macropinocytosis and phagocytosis by macrophages. *J. Cell Biol.* **135**, 1249-1260.

Barreiro, O., Yanez-Mo, M., Serrador, J. M., Montoya, M. C., Vicente-Manzanares, M., Tejedor, R., Furthmayr, H. and Sanchez-Madrid, F. (2002). Dynamic interaction of VCAM-1 and ICAM-1 with moesin and ezrin in a novel endothelial docking structure for adherent leukocytes. *J. Cell Biol.* **157**, 1233-1245.

Bretscher, A., Reczek, D. and Berryman, M. (1997). Ezrin: a protein requiring conformational activation to link microfilaments to the plasma membrane in the assembly of cell surface structures. *J. Cell Sci.* **110**, 3011-3018.

Brown, S., Heinisch, I., Ross, E., Shaw, K., Buckley, C. D. and Savill, J. (2002). Apoptosis disables CD31-mediated cell detachment from phagocytes promoting binding and engulfment. *Nature* **418**, 200-203.

Cao, T. T., Deacon, H. W., Reczek, D., Bretscher, A. and von Zastrow, M. (1999). A kinase-regulated PDZ-domain interaction controls endocytic sorting of the beta2-adrenergic receptor. *Nature* **401**, 286-290.

Caron, E. and Hall, A. (2001). Phagocytosis. In *Endocytosis* (ed. M. Marsh), pp. 58-77. Oxford: Oxford University Press.

Carpen, O., Pallai, P., Staunton, D. E. and Springer, T. A. (1992). Association of intercellular adhesion molecule-1 (ICAM-1) with actin-containing cytoskeleton and alpha-actinin. *J. Cell Biol.* **118**, 1223-1234.

Cox, D., Tseng, C. C., Bjekic, G. and Greenberg, S. (1999). A requirement for phosphatidylinositol 3-kinase in pseudopod extension. *J. Biol. Chem.* **274**, 1240-1247.

Danilov, S. M., Gavrilyuk, V. D., Franke, F. E., Pauls, K., Harshaw, D. W., McDonald, T. D., Miletich, D. J. and Muzykantov, V. R. (2001). Lung uptake of antibodies to endothelial antigens: key determinants of vascular immunotargeting. *Am. J. Physiol. Lung Cell. Mol. Physiol.* **280**, L1335-1347.

DeLisser, H. M. and Albelda, S. M. (1998). The function of cell adhesion molecules in lung inflammation: more questions than answers. *Am. J. Respir. Cell Mol. Biol.* **19**, 533-536.

Denker, S. P., Huang, D. C., Orlowski, J., Furthmayr, H. and Barber, D. L. (2000). Direct binding of the Na–H exchanger NHE1 to ERM proteins regulates the cortical cytoskeleton and cell shape independently of H(+) translocation. *Mol. Cell* **6**, 1425-1436.

Edgell, C. J., McDonald, C. C. and Graham, J. B. (1983). Permanent cell line expressing human factor VIII-related antigen established by hybridization. *Proc. Natl. Acad. Sci. USA* **80**, 3734-3737.

Etienne, S., Adamson, P., Greenwood, J., Strosberg, A. D., Cazaubon, S. and Couraud, P. O. (1998). ICAM-1 signaling pathways associated with Rho activation in microvascular brain endothelial cells. *J. Immunol.* **161**, 5755-5761.

Etienne-Manneville, S., Manneville, J. B., Adamson, P., Wilbourn, B., Greenwood, J. and Couraud, P. O. (2000). ICAM-1-coupled cytoskeletal rearrangements and transendothelial lymphocyte migration involve intracellular calcium signaling in brain endothelial cell lines. *J. Immunol.* **165**, 3375-3383.

Farsad, K., Ringstad, N., Takei, K., Floyd, S. R., Rose, K. and De Camilli, P. (2001). Generation of high curvature membranes mediated by direct endophilin bilayer interactions. *J. Cell Biol.* **155**, 193-200.

Fiorentini, C., Falzano, L., Fabbri, A., Stringaro, A., Logozzi, M., Travaglione, S., Contamin, S., Arancia, G., Malorni, W. and Fais, S. (2001). Activation of rho GTPases by cytotoxic necrotizing factor 1 induces macropinocytosis and scavenging activity in epithelial cells. *Mol. Biol. Cell* **12**, 2061-2073.

Fujimoto, L. M., Roth, R., Heuser, J. E. and Schmid, S. L. (2000). Actin assembly plays a variable, but not obligatory role in receptor- mediated endocytosis in mammalian cells. *Traffic* **1**, 161-171.

Gaietta, G., Deerinck, T. J., Adams, S. R., Bouwer, J., Tour, O., Laird, D. W., Sosinsky, G. E., Tsien, R. Y. and Ellisman, M. H. (2002). Multicolor and electron microscopic imaging of connexin trafficking. *Science* **296**, 503-507.

Gold, E. S., Underhill, D. M., Morrissette, N. S., Guo, J., McNiven, M. A. and Aderem, A. (1999). Dynamin 2 is required for phagocytosis in macrophages. *J. Exp. Med.* **190**, 1849-1856.

Grimmer, S., Van Deurs, B. and Sandvig, K. (2002). Membrane ruffling and macropinocytosis in A431 cells require cholesterol. *J. Cell Sci.* **115**, 2953-2962.

Hansen, S. H., Sandvig, K. and van Deurs, B. (1993). Clathrin and HA2 adaptors: effects of potassium depletion, hypertonic medium, and cytosol acidification. *J. Cell Biol.* **121**, 61-72.

Heiska, L., Alfthan, K., Gronholm, M., Vilja, P., Vaheri, A. and Carpen, O. (1998). Association of ezrin with intercellular adhesion molecule-1 and -2 (ICAM-1 and ICAM-2). Regulation by phosphatidylinositol 4,5-bisphosphate. *J. Biol. Chem.* **273**, 21893-21900.

Henley, J. R., Krueger, E. W., Oswald, B. J. and McNiven, M. A. (1998). Dynamin-mediated internalization of caveolae. *J. Cell Biol.* **141**, 85-99.

Hirao, M., Sato, N., Kondo, T., Yonemura, S., Monden, M., Sasaki, T., Takai, Y. and Tsukita, S. (1996). Regulation mechanism of ERM (ezrin/radixin/moesin) protein/plasma membrane association: possible involvement of phosphatidylinositol turnover and Rho-dependent signaling pathway. *J. Cell Biol.* **135**, 37-51.

Jacobson, B. S., Stolz, D. B. and Schnitzer, J. E. (1996). Identification of endothelial cell-surface proteins as targets for diagnosis and treatment of disease. *Nat. Med.* **2**, 482-484.

Johnson-Leger, C., Aurrand-Lions, M. and Imhof, B. A. (2000). The parting of the endothelium: miracle, or simply a junctional affair? *J. Cell Sci.* **113**, 921-933.

Jordan, K., Chodock, R., Hand, A. R. and Laird, D. W. (2001). The origin of annular junctions: a mechanism of gap junction internalization. *J. Cell Sci.* **114**, 763-773.

Koval, M., Preiter, K., Adles, C., Stahl, P. D. and Steinberg, T. H. (1998). Size of IgG-opsonized particles determines macrophage response during internalization. *Exp. Cell Res.* **242**, 265-273.

Lamaze, C. and Schmid, S. L. (1995). The emergence of clathrin-independent pinocytic pathways. *Curr. Opin. Cell Biol.* **7**, 573-580.

Larsen, E. C., DiGennaro, J. A., Saito, N., Mehta, S., Loegering, D. J., Mazurkiewicz, J. E. and Lennartz, M. R. (2000). Differential requirement for classic and novel PKC isoforms in respiratory burst and phagocytosis in RAW 264.7 cells. *J. Immunol.* **165**, 2809-2817.

Lee, E. and Knecht, D. A. (2002). Visualization of actin dynamics during macropinocytosis and exocytosis. *Traffic* **3**, 186-192.

Lee, A., Frank, D. W., Marks, M. S. and Lemmon, M. A. (1999). Dominant-negative inhibition of receptor-mediated endocytosis by a dynamin-1 mutant with a defective pleckstrin homology domain. *Curr. Biol.* **9**, 261-264.

Li, S., Tan, Y., Viroonchatapan, E., Pitt, B. R. and Huang, L. (2000). Targeted gene delivery to pulmonary endothelium by anti-PECAM antibody. *Am. J. Physiol. Lung Cell. Mol. Physiol.* **278**, L504-511.

Liu, N. Q., Lossinsky, A. S., Popik, W., Li, X., Gujuluva, C., Kriederman, B., Roberts, J., Pushkarsky, T., Bukrinsky, M., Witte, M. et al. (2002). Human immunodeficiency virus type 1 enters brain microvascular endothelia by macropinocytosis dependent on lipid rafts and the mitogen-activated protein kinase signaling pathway. *J. Virol.* **76**, 6689-6700.

Mayor, S., Sabharanjak, S. and Maxfield, F. R. (1998). Cholesterol-dependent retention of GPI-anchored proteins in endosomes. *EMBO J.* **17**, 4626-4638.

McIntosh, D. P., Tan, X. Y., Oh, P. and Schnitzer, J. E. (2002). Targeting endothelium and its dynamic caveolae for tissue-specific transcytosis in vivo: a pathway to overcome cell barriers to drug and gene delivery. *Proc. Natl. Acad. Sci. USA* **99**, 1996-2001.

Minshall, R. D., Tiruppathi, C., Vogel, S. M., Niles, W. D., Gilchrist, A., Hamm, H. E. and Malik, A. B. (2000). Endothelial cell-surface gp60 activates vesicle formation and trafficking via G(i)-coupled Src kinase signaling pathway. *J. Cell Biol.* **150**, 1057-1070.

Mukherjee, S., Ghosh, R. N. and Maxfield, F. R. (1997). Endocytosis. *Physiol. Rev.* **77**, 759-803.

Muzykantov, V. R., Atochina, E. N., Ischiropoulos, H., Danilov, S. M. and

Fisher, A. B. (1996). Immunotargeting of antioxidant enzyme to the pulmonary endothelium. *Proc. Natl. Acad. Sci. USA* **93**, 5213-5218.

Muzykantov, V. R., Christofidou-Solomidou, M., Balyasnikova, I., Harshaw, D. W., Schultz, L., Fisher, A. B. and Albelda, S. M. (1999). Streptavidin facilitates internalization and pulmonary targeting of an anti-endothelial cell antibody (platelet-endothelial cell adhesion molecule 1): a strategy for vascular immunotargeting of drugs. *Proc. Natl. Acad. Sci. USA* **96**, 2379-2384.

Nichols, B. J. and Lippincott-Schwartz, J. (2001). Endocytosis without clathrin coats. *Trends Cell Biol.* **11**, 406-412.

Olazabal, I. M., Caron, E., May, R. C., Schilling, K., Knecht, D. A. and Machesky, L. M. (2002). Rho-kinase and myosin-II control phagocytic cup formation during CR, but not FcgammaR, phagocytosis. *Curr. Biol.* **12**, 1413-1418.

Orth, J. D., Krueger, E. W., Cao, H. and McNiven, M. A. (2002). The large GTPase dynamin regulates actin comet formation and movement in living cells. *Proc. Natl. Acad. Sci. USA* **99**, 167-172.

Parton, R. G., Joggerst, B. and Simons, K. (1994). Regulated internalization of caveolae. *J. Cell Biol.* **127**, 1199-1215.

Powell, K. A., Valova, V. A., Malladi, C. S., Jensen, O. N., Larsen, M. R. and Robinson, P. J. (2000). Phosphorylation of dynamin I on Ser-795 by protein kinase C blocks its association with phospholipids. *J. Biol. Chem.* **275**, 11610-11617.

Predescu, D., Predescu, S., McQuistan, T. and Palade, G. E. (1998). Transcytosis of alpha1-acidic glycoprotein in the continuous microvascular endothelium. *Proc. Natl. Acad. Sci. USA* **95**, 6175-6180.

Puri, V., Watanabe, R., Singh, R. D., Dominguez, M., Brown, J. C., Wheatley, C. L., Marks, D. L. and Pagano, R. E. (2001). Clathrin-dependent and -independent internalization of plasma membrane sphingolipids initiates two Golgi targeting pathways. *J. Cell Biol.* **154**, 535-547.

Putney, L. K., Denker, S. P. and Barber, D. L. (2002). The changing face of the Na+/H+ exchanger, NHE1: structure, regulation, and cellular actions. *Annu. Rev. Pharmacol. Toxicol.* **42**, 527-552.

Racoosin, E. L. and Swanson, J. A. (1989). Macrophage colony-stimulating factor (rM-CSF) stimulates pinocytosis in bone marrow-derived macrophages. *J. Exp. Med.* **170**, 1635-1648.

Racoosin, E. L. and Swanson, J. A. (1992). M-CSF-induced macropinocytosis increases solute endocytosis but not receptor-mediated endocytosis in mouse macrophages. *J. Cell Sci.* **102**, 867-880.

Sahai, E. and Marshall, C. J. (2002). ROCK and Dia have opposing effects on adherens junctions downstream of Rho. *Nat. Cell Biol.* **4**, 408-415.

Scherpereel, A., Rome, J. J., Wiewrodt, R., Watkins, S. C., Harshaw, D. W., Alder, S., Christofidou-Solomidou, M., Haut, E., Murciano, J. C., Nakada, M. et al. (2002). Platelet-endothelial cell adhesion molecule-1-directed immunotargeting to cardiopulmonary vasculature. *J. Pharmacol. Exp. Ther.* **300**, 777-786.

Scherpereel, A., Wiewrodt, R., Christofidou-Solomidou, M., Gervais, R., Murciano, J. C., Albelda, S. M. and Muzykantov, V. R. (2001). Cell-selective intracellular delivery of a foreign enzyme to endothelium in vivo using vascular immunotargeting. *FASEB J.* **15**, 416-426.

Schlegel, R., Dickson, R. B., Willingham, M. C. and Pastan, I. H. (1982). Amantadine and dansylcadaverine inhibit vesicular stomatitis virus uptake and receptor-mediated endocytosis of alpha 2-macroglobulin. *Proc. Natl. Acad. Sci. USA* **79**, 2291-2295.

Schnitzer, J. E., Oh, P., Pinney, E. and Allard, J. (1994). Filipin-sensitive caveolae-mediated transport in endothelium: reduced transcytosis, scavenger endocytosis, and capillary permeability of select macromolecules. *J. Cell Biol.* **127**, 1217-1232.

Schubert, W., Frank, P. G., Razani, B., Park, D. S., Chow, C. W. and Lisanti, M. P. (2001). Caveolae-deficient endothelial cells show defects in the uptake and transport of albumin in vivo. *J. Biol. Chem.* **276**, 48619-48622.

Shafren, D. R., Dorahy, D. J., Greive, S. J., Burns, G. F. and Barry, R. D. (1997a). Mouse cells expressing human intercellular adhesion molecule-1 are susceptible to infection by coxsackievirus A21. *J. Virol.* **71**, 785-789.

Shafren, D. R., Dorahy, D. J., Ingham, R. A., Burns, G. F. and Barry, R. D. (1997b). Coxsackievirus A21 binds to decay-accelerating factor but requires intercellular adhesion molecule 1 for cell entry. *J. Virol.* **71**, 4736-4743.

Skretting, G., Torgersen, M. L., van Deurs, B. and Sandvig, K. (1999). Endocytic mechanisms responsible for uptake of GPI-linked diphtheria toxin receptor. *J. Cell Sci.* **112**, 3899-3909.

Spragg, D. D., Alford, D. R., Greferath, R., Larsen, C. E., Lee, K. D., Gurtner, G. C., Cybulsky, M. I., Tosi, P. F., Nicolau, C. and Gimbrone, M. A., Jr (1997). Immunotargeting of liposomes to activated vascular endothelial cells: a strategy for site-selective delivery in the cardiovascular system. *Proc. Natl. Acad. Sci. USA* **94**, 8795-8800.

Swanson, J. A. (1989). Phorbol esters stimulate macropinocytosis and solute flow through macrophages. *J. Cell Sci.* **94**, 135-142.

Swanson, J. A. and Watts, C. (1995). Macropinocytosis. *Trends Cell Biol.* **5**, 424-428.

Thompson, P. W., Randi, A. M. and Ridley, A. J. (2002). Intercellular adhesion molecule (ICAM)-1, but not ICAM-2, activates RhoA and stimulates c-fos and rhoA transcription in endothelial cells. *J. Immunol.* **169**, 1007-1013.

Torgersen, M. L., Skretting, G., van Deurs, B. and Sandvig, K. (2001). Internalization of cholera toxin by different endocytic mechanisms. *J. Cell Sci.* **114**, 3737-3747.

Treutiger, C. J., Heddini, A., Fernandez, V., Muller, W. A. and Wahlgren, M. (1997). PECAM-1/CD31, an endothelial receptor for binding *Plasmodium falciparum*-infected erythrocytes. *Nat. Med.* **3**, 1405-1408.

Volberg, T., Geiger, B., Citi, S. and Bershadsky, A. D. (1994). Effect of protein kinase inhibitor H-7 on the contractility, integrity, and membrane anchorage of the microfilament system. *Cell Motil. Cytoskeleton* **29**, 321-338.

Wang, Q. and Doerschuk, C. M. (2002). The signaling pathways induced by neutrophil-endothelial cell adhesion. *Antioxid. Redox Signal* **4**, 39-47.

Watanabe, T., Pakala, R., Katagiri, T. and Benedict, C. R. (2001). Synergistic effect of urotensin II with mildly oxidized LDL on DNA synthesis in vascular smooth muscle cells. *Circulation* **104**, 16-18.

West, M. A., Bretscher, M. S. and Watts, C. (1989). Distinct endocytotic pathways in epidermal growth factor-stimulated human carcinoma A431 cells. *J. Cell Biol.* **109**, 2731-2739.

West, M. A., Prescott, A. R., Eskelinen, E. L., Ridley, A. J. and Watts, C. (2000). Rac is required for constitutive macropinocytosis by dendritic cells but does not control its downregulation. *Curr. Biol.* **10**, 839-848.

Wiewrodt, R., Thomas, A. P., Cipelletti, L., Christofidou-Solomidou, M., Weitz, D. A., Feinstein, S. I., Schaffer, D., Albelda, S. M., Koval, M. and Muzykantov, V. R. (2002). Size-dependent intracellular immunotargeting of therapeutic cargoes into endothelial cells. *Blood* **99**, 912-922.

Witke, W., Podtelejnikov, A. V., Di Nardo, A., Sutherland, J. D., Gurniak, C. B., Dotti, C. and Mann, M. (1998). In mouse brain profilin I and profilin II associate with regulators of the endocytic pathway and actin assembly. *EMBO J.* **17**, 967-976.

Worthylake, R. A. and Burridge, K. (2001). Leukocyte transendothelial migration: orchestrating the underlying molecular machinery. *Curr. Opin. Cell Biol.* **13**, 569-577.